ICARUS 5, 237–244 (1966)

Solar and Lunar Observations at Submillimeter Wavelengths

JOHN N. GAITSKELL AND ANTHONY E. GEAR

Department of Physics, Queen Mary College, University of London, London, England

Communicated by Zdeněk Kopal

Received August 15, 1965

Observations of solar radiation in the spectral range 200 to 2000 microns are described. A Fabry-Perot interferometer with metal meshes as reflecting elements was used as a wavelength scanning device in first-order transmission. The observations were carried out at an altitude of 2880 meters from the Pic-du-Midi Observatory. Some preliminary submillimeter lunar equatorial transits using the Fabry-Perot interferometer as an interference filter centered on a wavelength of 740 microns are also described.

Introduction

The atmospherically attenuated solar spectrum has been studied at submillimeter wavelengths by Gebbie (1957) using a Michelson interferometer and by Averkov *et al.* (1964) using a grating spectrometer. The present paper describes the development of a Fabry-Perot interferometer (FPI) for use in conjunction with a telescope for submillimeter atmospheric and astrophysical observations, the compactness and relatively high luminosity of this type of instrument making it well suited for this work. Two-dimensional metal grids were used as the reflecting elements of the interferometer, this technique having been investigated experimentally by Renk and Genzel (1962) and theoretically (in the case of one-dimensional grids) by Casey and Lewis (1952). The use of grids is preferable to that of homogeneous metal films for work in the submillimeter region in that it is possible, with appropriate choice of grid constants, to combine the requirements of high peak transmission with high finesse, whereas the two cannot simultaneously be achieved if metal films are used at these wavelengths. If the interferometer is used in first order, so that between the short wavelength cutoff value, defined by the filtering material used, and twice this wavelength there is no overlapping of transmission orders, the spectrum may be obtained directly. The interferometer may be used astrophysically either for spectroscopic scanning or as a fixed spacing etalon for source scanning in a chosen, well-defined, spectral band.

Instrumentation

The FPI was placed in front of a broadband Golay detector mounted at the focus of a 1.6-meter aperture Cassegrain telescope (Fig. 1) in order to augment the submillimeter component of the atmospherically transmitted solar spectrum, the telescope was mounted at the Pic-du-Midi observatory in the Pyrenees at an altitude of 2880 meters above sea level. This arrangement of the interferometer in front of the detector was only suitable for work with fairly low spectral resolving powers, i.e., up to about 30, due to the useful resolving power of the FPI being limited by the semiangle of the cone of radiation passing through it, this being approximately 15°.

In order to record the atmospherically transmitted solar spectrum, the interferometer plate separation was increased linearly from zero, while the polar-mounted

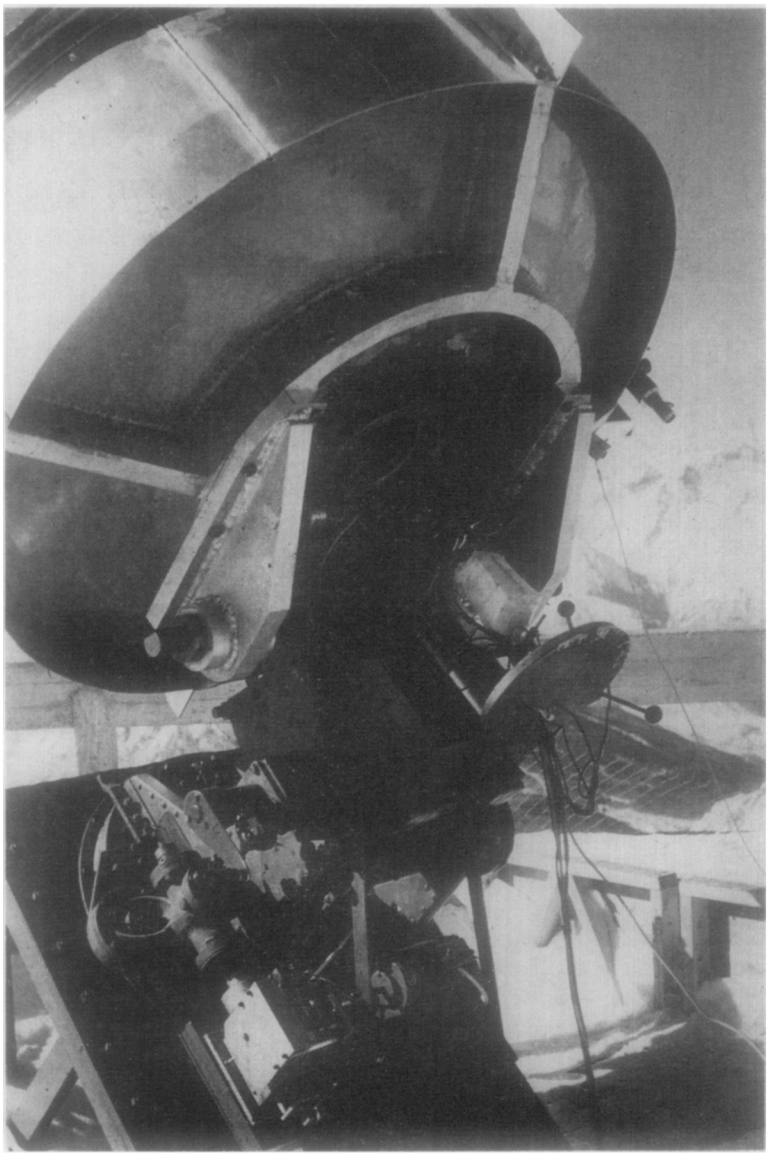

FIG. 1. The 1.6-meter aperture Cassegrain telescope mounted at the Pic-du-Midi Observatory.

telescope tracked on the center of the optical solar disk. Synchronous electric motors and reduction gear trains were used for both driving motions.

Two-dimensional, rectangular cross-section, unsupported nickel grids were used as the reflecting elements of the interferometer. Each of these was glued to a brass annulus and tautened using an inner brass ring pressed into contact with the grid by means of adjusting screws. In this way the grids were maintained plane to at least ± 3 microns. The grid interval, g, used for the observations was 211 microns, while the ratio of this grid interval to the half-width of the grid strips, a, was 8. The grid thickness was 8 microns which is much greater than the penetration depth of the radiation in the wavelength range of the observations.

A theoretical expression for the half-value width, $\Delta\lambda$, of the FPI transmission band centered on a wavelength λ, in first

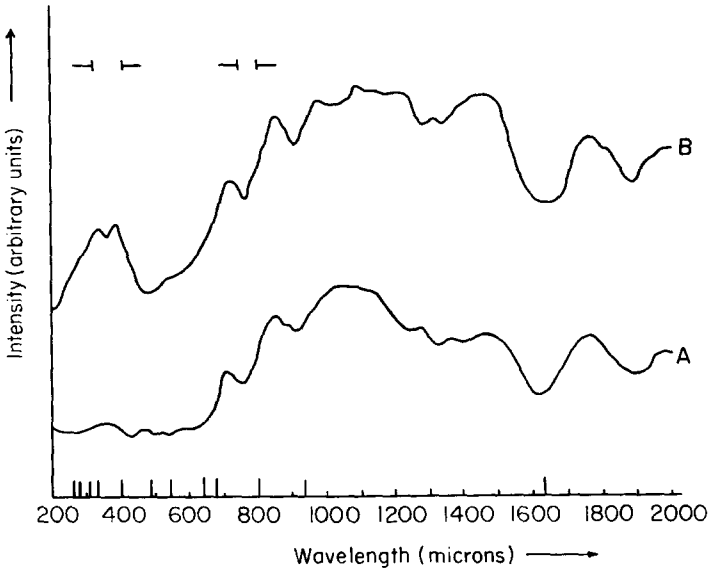

FIG. 2. Two Fabry-Perot solar interferographs, each the mean of five spectral runs. Curve A was obtained using 1.5 cm of sooted polythene filtering material, while curve B was obtained using 1.5 mm of restrahlen absorption filtering, two thicknesses of black, polythene-backed, photographic paper also being used in each case. The widths of the FPI passband to half-peak transmission values at 400 and 800 microns are indicated on the figure. Also shown as short vertical lines are the positions of the principal absorption lines due to water vapor.

order has been given by Ulrich *et al.* (1963) for the case of a normally incident parallel beam

$$\Delta\lambda_1 = \frac{4w^2g^2}{\pi\lambda_1}\left(1 + \frac{4w^2g^2}{\lambda_1^2}\right)^{-1/2}, \qquad (1)$$

where $w = \ln \csc(\pi a/g)$, and absorption in the grids is neglected. The wavelength, λ_1, of peak transmission in first order is given by

$$\lambda_1 = 2(d + c). \qquad (2)$$

In this equation d is the separation of the reflecting plates. The parameter c is a constant, independent of wavelength, and is introduced in order to take account of the fact that the change of phase at each reflection at a grid is not exactly π. For the grids used this constant was determined by a separate calibrating experiment using an 8-mm wavelength source.

The interferometer was used in first-order transmission, conventional absorption filtering being used to reduce unwanted $\lambda_1/2$ radiation appearing in second order. By using different filtering materials and thicknesses, it was found possible to study different submillimeter spectral ranges. Thicknesses of up to 1.5 cm of soot-impregnated polythene, and up to 1.5 mm of restrahlen absorption filtering (Yamada *et al.*, 1962) were found especially useful for investigating the regions from 500 to 1000 microns, and from 250 to 500 microns, respectively. Figure 2 demonstrates the effect on the observed spectra of the use of different filtering materials. These spectra were obtained in December when the solar elevation never exceeded 20° and the submillimeter component was already highly attenuated by the atmosphere. The filtering material was fitted into the radiation-condensing nose cone of the detector.

EXPERIMENTAL PROCEDURE AND RESULTS

In order to obtain an estimate of the absorption coefficient of atmospheric water vapor as a function of wavelength in the region 200–1000 microns, a series of spectra were recorded at different solar elevations on 9 March 1965. The telescope was driven

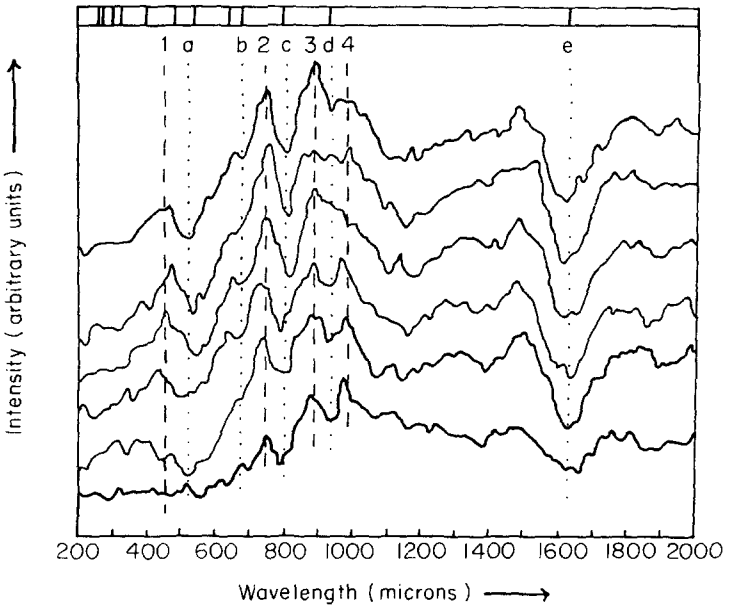

FIG. 3. A series of Fabry-Perot interferographs obtained on the same day. The positions of the principal absorption lines due to water vapor are shown at the top of the figure. The dashed vertical lines numbered 1 to 4 mark the mean positions of the four principal transmission regions observed while the letters a to e mark the mean positions of the observed absorption lines. The lowest trace on the figure was obtained with a low solar elevation compared with the upper five, which were obtained near noon. This trace differs from the others in that the 480-micron transmission region is absent.

at solar rate, while the FPI plates were driven apart uniformly from zero separation so as to scan the required spectral region, this procedure being repeated throughout the day. In order to obtain a reference zero level for the spectral intensities, the signal level from a region of sky adjacent to the Sun was measured before each run with the etalon spacing zero, and after each run with the etalon spacing as at the end of the run. The line joining the mean of these two levels was then taken as the reference zero level, a check being made by a separate interferograph completely on sky, which was found to be linear with the sensitivity available. A thick (1.5-cm) sooted polythene filter was used so that wavelengths below 500 microns were appreciably attenuated, although not completely, as can be seen from Fig. 3 which shows five interferographs obtained near noon, together with one near sunset for comparison.

The numbers 1 to 4 and letters a to e on Fig. 3 refer to the principal spectral features which appear. Below 1 mm overlapping of orders is not appreciable due to the filtering minimizing radiation below 500 microns and will be neglected. (The presence of the peak near 880 microns on spectra obtained at low altitude indicates that it is not due to second order of the peak near 450 microns as this is absent on these spectra.) Above 1 mm overlapping of orders becomes appreciable but feature e stands out clearly on all traces and coincides well with the strong water-vapor absorption line at 1.63 mm, already observed in the atmospherically attenuated solar spectrum by Bastin *et al.* (1964). The features marked 1 to 4 indicate regions of relatively high atmospheric transmission centered on wavelengths 450, 740, 880, and 980 microns, respectively, while features a to e are regions of absorption, region b being barely resolved. These wavelengths correspond well with the principal trans-

mission and absorption regions in the theoretically calculated water-vapor absorption curve, the positions of the calculated absorption peaks being shown by the vertical lines along the wavelength axis. In the case of the transmission regions mentioned, the absorption coefficient did not vary appreciably over the half-value width of the FPI transmission band, so that a rough estimate of the relative absorption coefficients in these regions could be deduced.

In order to obtain this estimate, the following simplifying assumptions were made:

(1) The value of the mass absorption coefficient, k_λ, is constant with height and temperature and is, therefore, independent of the particular distribution of water vapor in the atmosphere.

(2) The FPI etalon can be regarded as a narrow band filter, only transmitting radiation in a wavelength range comparable with the half-value width of the FPI first-order transmission band.

(3) For each of the atmospheric transmission regions considered, the value of k_λ is only slowly varying with wavelength and may usefully be replaced by a mean absorption coefficient, $\bar{k}_n$, averaged over the range of wavelengths in the FPI passband centered on λ_n, the effective wavelength of peak transmission of the nth region.

The intensity I_n of the signal detected by the telescope may then be written

$$I_n = B_n \exp\{-\bar{k}_n m \csc\theta(t)\}, \quad (3)$$

where the function B_n depends upon the intensity of the solar source and the performance of the telescope, filters, and detector for wavelengths near λ_n, but is independent of the atmospheric conditions; m is an effective precipitable water-vapor density averaged over height in the atmosphere, and $\theta(t)$ is the solar altitude at the time of observation (t). This equation is derived in Bastin *et al.* (1964). If further we assume that $m \csc\theta(t)$ does not change significantly while scanning through two adjacent transmission bands, we may write

$$I_{n+1} = B_{n+1} \exp\{-\bar{k}_{n+1} m \csc\theta(t)\}. \quad (4)$$

Taking the logarithms of (3) and (4) and dividing, it is seen that

$$\frac{\ln I_{n+1} - \ln B_{n+1}}{\ln I_n - \ln B_n} = \frac{\bar{k}_{n+1}}{\bar{k}_n}.$$

Hence,

$$\ln I_{n+1}(t) = (\bar{k}_{n+1}/\bar{k}_n) \ln I_n(t) + C, \quad (5)$$

where C is independent of time. In accordance with Eq. (5), plots of $\log I_{n+1}$ against $\log I_n$ for spectra obtained at different times during the day were made, as shown in Fig. 4. So as to justify the assumption that $\csc\theta(t)$ was essentially unchanged while the FPI scanned from one transmission peak to the next, spectra obtained for values of $\theta(t)$ less than about 8° were omitted from the analysis. The graphs are reasonably linear, the estimates of errors shown being those due to the detector noise of the system, while the spread of points indicates superposed fluctuations probably due primarily to rapid local changes in atmospheric conditions.

From the slopes of the best fitting straight lines through the experimental points of Fig. 4, and using Eq. (5), the values of relative absorption coefficients obtained were as follows:

$$\bar{k}_2/\bar{k}_1 = 0.43 \pm 0.09; \quad \bar{k}_3/\bar{k}_2 = 0.73 \pm 0.9; \quad \bar{k}_4/\bar{k}_3 = 0.76 \pm 0.07. \quad (6)$$

It must be emphasized that the assumptions made in the derivation of Eq. (6) imply that the experimental ratios of the absorption coefficients given by Eq. (4) apply to effective absorption coefficients averaged over the passband of the interferometer when centered on each relative transmission band, and also averaged over height in the atmosphere. A quantitative comparison of these ratios with theoretical estimates would require a detailed knowledge of the instrumental function of the FPI and also of the thermodynamic properties of the atmosphere as regards water vapor. Theoretical values for the ratios of the absorption coefficients at the four wavelengths (at 300°K and 1 atm pressure) have been made available to us by Dr.

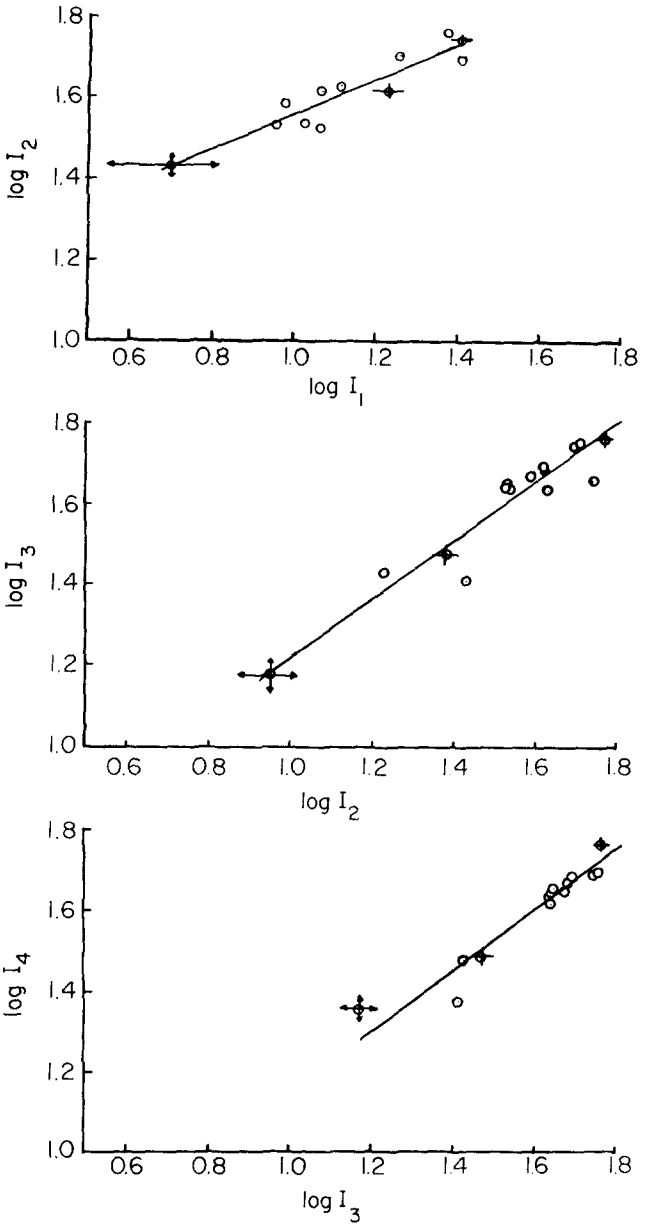

FIG. 4. Logarithm of intensity (arb. units) at wavelength λ_n plotted against logarithm of intensity (same arb. units) at wavelength λ_{n+1}, for the four wavelengths of relatively high atmospheric transmission.

P. E. Clegg (private communication). These ratios are

$$k_2/k_1 = 0.58; \quad k_3/k_2 = 0.83; \quad k_4/k_3 = 0.91. \tag{7}$$

LUNAR SUBMILLIMETER OBSERVATIONS

Preliminary lunar scans at submillimeter wavelengths have been made during a period of favorable weather conditions. The FPI plates were adjusted to a separation to give peak transmission at a wavelength $\lambda = 740$ microns in first order. This wavelength was chosen to coincide with an atmospheric transmission peak found from observations described in the previous section.

FIG. 5. Mean of six equatorial lunar scans at a wavelength $\lambda = 740$ microns, taken at regularly spaced sampling points. The phase was 4 days after new moon, and the positions of first and last limbs crossing the telescope axis are shown by the short vertical lines.

Using the interferometer as a fixed etalon, a series of six lunar scans were recorded during a 2-hr observational period. The mean resultant scan, found from superposing the individual scans is shown in Fig. 5. The observations were made 4 days after new moon.

Solar signals obtained on previous days at the same wavelength, and radiosonde atmospheric data have been used in order to obtain an estimate of lunar temperature. If a solar brightness temperature of 5500°K is adopted, the lunar brightness temperature (approximately disc averaged) may be evaluated, giving 340° ± 50°K at a phase angle of 234° from full moon, and at a mean wavelength of $\lambda = 740$ microns. The random error quoted above is, however, small compared with the systematic error introduced at the analysis stage by the use of radiosonde data from stations at some distance from the observation site, this data being found to vary considerably between simultaneous ascents made at the three nearest stations. When this additional source of error is considered, the lunar temperature estimate given here is not inconsistently high when compared with previous observations at longer and shorter wavelengths. The use of the "equal altitude" method of comparing solar and lunar signals (Bastin *et al.*, 1964) should lead to a much more reliable estimate of the ratio of solar to lunar brightness temperature at this and other submillimeter wavelengths.

CONCLUSIONS

Fabry-Perot interferometers appear to be particularly useful for astrophysical spectroscopic scanning work at submillimeter wavelengths because of their compactness combined with relatively high peak transmission and resolving power compared with the more conventional grating spectrometers. FPI's are also ideally suited to source drift-scanning in narrow spectral bands whereas Michelson interferometers cannot be used in this manner in order to build up brightness contours of extended sources.

From high-altitude sites, or balloon platforms, useful submillimeter observations of the Sun and Moon are quite feasible, using

an FPI etalon as a narrow band filter. For such work at high altitudes efficient auxiliary long-wavelength pass filters need to be developed. To accomplish this it may be possible to incorporate into the telescope design filtering techniques depending on the reflection properties of plane, two-dimensional, grids of circular wires or a second interference filter used in reflection.

Quite detailed brightness distributions over the solar and lunar discs may be obtained at submillimeter wavelengths with relatively small aperture telescopes. For example, a 1-meter telescope working at 200-micron wavelength can theoretically resolve angular detail of about one minute of arc, or $\frac{1}{30}$th of the angular size of the Sun or Moon.

NOTES ADDED IN PROOF:

(1) A redetermination of the constant c appearing in Eq. (2) has been made at 750 microns. Taking this into account as well as the small correction for the shift of peak transmission due to finite beam angle, it has been found that all quoted wavelengths and wavelength scales require reduction by 30 microns, the residual probable error in wavelength then being ± 25 microns. The authors wish to thank Dr. P. H. Knapp and Mr. R. Emery for providing the Froome-type harmonic generator used in this calibration.

(2) A more recent set of observations to determine lunar brightness temperature was obtained at the Pic-du-Midi Observatory on October 27, 1965, using the "equal altitude" method. Preliminary analysis gives a brightness temperature of $145° \pm 40°$K at 900 microns (corrected) wavelength, with the telescope centered on the Moon. The phase was 217° after full moon, and the telescope had a beam width of 18 minutes of arc to half-power points. This measurement is in good agreement with an interpolation between previous microwave and infrared data.

ACKNOWLEDGMENT

We wish to thank Professor J. Rösch and the staff of the Pic-du-Midi Observatory for allowing the use of the high altitude site and for a great deal of assistance in connection with the installation of the telescope. We are grateful to Dr. J. A. Bastin and Dr. P. E. Clegg for many useful suggestions, and to Professor G. O. Jones for a great deal of help and encouragement in connection with this project.

REFERENCES

AVERKOV, S. I., ANIKIN, V. I., RYADOV, V. YA., AND FURASHOV, N. I. (1964). Astronomical station for far-infrared observations. *Soviet Astron.—AJ (English Transl.)* **8**, 432.

BASTIN, J. A., GEAR, A. E., JONES, G. O., SMITH, H. J. T., AND WRIGHT, P. J. (1964). Spectroscopy at extreme infrared wavelengths III. Astrophysical and atmospheric measurements. *Proc. Roy. Soc. (London)* **A278**, 543.

CASEY, J. P., AND LEWIS, E. A. (1952). Interferometer action of a parallel pair of wire gratings. *J. Opt. Soc. Am.* **42**, 971.

GEBBIE, H. A. (1957). Detection of submillimeter solar radiation. *Phys. Rev.* **107**, 1194.

RENK, K. F., AND GENZEL, L. (1962). Interference filters and Fabry-Perot interferometers for the far infrared. *Appl. Optics.* **1**, 643.

ULRICH, R., RENK, K. F., AND GENZEL, L. (1963). Tunable submillimeter interferometers of the Fabry-Perot type. *IEEE (Inst. Elec. Electron. Eng.) Trans. Microwave Theory Tech.* **11**, 363.

YAMADA, Y., MITSUISHI, A., AND YOSHINAGA, H. (1962). Transmission filters in the far-infrared region. *J. Opt. Soc. Am.* **52**, 17.